End plate biasing experiments in linear magnetized plasmas

2014 Nucl. Fusion 54 114010

(http://iopscience.iop.org/0029-5515/54/11/114010)

IOP Publishing | International Atomic Energy Agency Nuclear Fusion
Nucl. Fusion **54** (2014) 114010 (5pp) doi:10.1088/0029-5515/54/11/114010

End plate biasing experiments in linear magnetized plasmas

T. Yamada[1,2], S. Inagaki[2,3], T. Kobayashi[4], Y. Nagashima[2,3], T. Mitsuzono[4], Y. Miwa[4], K. Nakanishi[4], H. Fujino[4], M. Sasaki[2,3], N. Kasuya[2,3], M. Lesur[2], Y. Kosuga[3,5], A. Fujisawa[2,3], S.-I. Itoh[2,3] and K. Itoh[2,6]

[1] Faculty of Arts and Science, Kyushu University, Fukuoka 819-0395, Japan
[2] Itoh Research Center for Plasma Turbulence, Kyushu University, Kasuga 816-8580, Japan
[3] Research Institute for Applied Mechanics, Kyushu University, Kasuga 816-8580, Japan
[4] Interdisciplinary Graduate School of Engineering Sciences, Kyushu University, Kasuga 816-8580, Japan
[5] Institute for Advanced Study, Kyushu University, Fukuoka 812-8581, Japan
[6] National Institute for Fusion Science, Toki 509-5292, Japan

E-mail: takuma@artsci.kyushu-u.ac.jp

Received 15 December 2013, revised 29 January 2014
Accepted for publication 3 February 2014
Published 4 November 2014

Abstract

Meso-scale streamer has a radially elongated structure and is believed to enhance the radial transport. In order to study the control of the streamer, we demonstrated an end plate biasing to the streamer state in the PANTA linear plasma. During the end plate biasing, the electron density profile became more peaked, fluctuation was suppressed, the streamer structure was deconstructed, and the waveform became a periodic solitary state. The radial electric field only induced at around the end plate was found to play an important role for the streamer suppression.

Keywords: streamer, linear plasma, end plate biasing

1. Introduction

Study of meso-scale structures, such as streamers and zonal flows, has been an important subject for understanding anomalous transport in linear and toroidal plasmas [1]. Recently, a streamer structure was first found in a linear cylindrical plasma, LMD-U [2]. Its poloidally localized and radially elongated structure was confirmed by using multi-channel poloidal probe arrays. In addition, a certain wave named 'mediator', which had the same frequency and poloidal wave number as the envelope of the streamer structure, was found to be strongly nonlinearly coupled with drift wave turbulence and playing an important role for the streamer formation [3]. The streamer is considered to enhance radial heat transport and thus a method to control streamers is strongly required to improve the plasma confinement. In the PANTA linear plasma device, discharge conditions to observe the streamer have been clarified [4] and numerical study on the dynamical transition from the streamer to the other turbulent state has started [5].

Electrode-biasing experiments have been performed in tokamaks [6, 7], helical devices [8, 9] and linear machines [10–14]. The biasing method is considered to be one of the promising tools to control plasma turbulence through formations of radial electric field and its shear. Study of controlling the streamer was performed in the PANTA device by biasing the end plate. During the end plate biasing, the streamer was suppressed, the fluctuation level was reduced, and the electron density profile became more peaked.

2. Streamers in PANTA

The streamer structure was clearly observed for the first time in a linear plasma of the LMD-U experimental device [2]. The mediator playing an important role for the streamer formation was also found, and its two-dimensional phase structure was analysed [3]. The LMD-U linear plasma device was modified to the PANTA linear plasma device in 2009 [15, 16]. Both devices have almost the same properties, only but the axial (z) length of the vacuum vessel was changed from 3740 to 4000 mm. The inner diameter of the PANTA vacuum vessel is 450 mm. A linear plasma with a diameter of around 100–120 mm is created by a radio-frequency wave (3 kW/7 MHz) at the source region made of quartz tube with an inner diameter of 95 mm. The peak electron density and electron/ion temperature of the linear plasma are about $10^{19}\,\mathrm{m}^{-3}$ and 3 eV/0.1 eV, respectively.

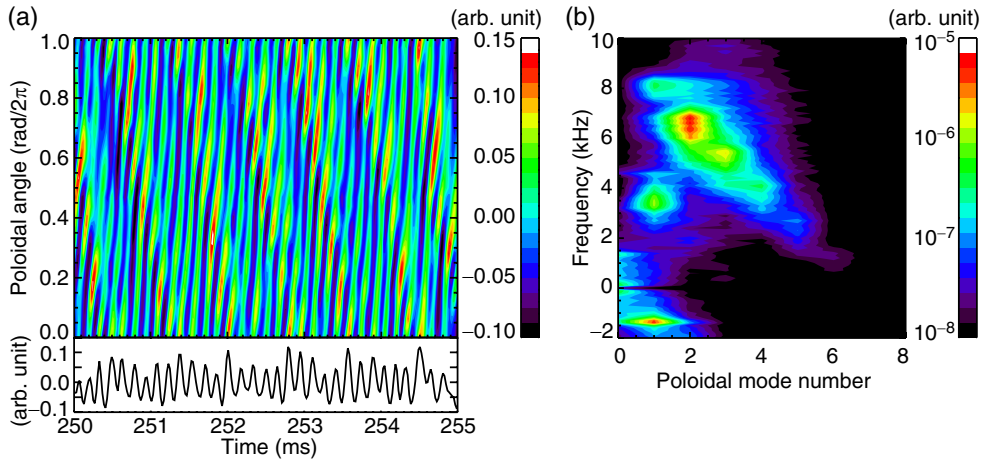

Figure 1. (*a*) Spatiotemporal waveform (with temporal waveform at $\theta = 0$) and (*b*) two-dimensional power spectrum of ion saturation-current fluctuation with discharge conditions; magnetic field of 0.09 T and argon pressure of 0.8 mTorr. Streamer structure is observed.

The steep electron density gradient at around the radius $r = 30$–40 mm produces resistive drift wave instabilities propagating in the positive poloidal direction θ, which is the electron diamagnetic drift direction, but the turbulent regime differs according to the discharge conditions, in our case, axial magnetic field and filling argon pressure at the source. In this paper, the ion saturation-current fluctuation, which reflects the electron density fluctuation, measured with a 64-channel poloidal Langmuir probe array [17] located at $r = 40$ mm and $z = 1885$ mm, was used for the turbulence and streamer study. When the magnetic field was under ~0.03 T, the spatiotemporal waveform of the ion saturation-current showed a coherent sine wave with a certain single poloidal mode number. Only a single instability mode with the certain poloidal mode number appeared in the two-dimensional (poloidal mode number–frequency) power spectrum. When the argon pressure was over ~3 mTorr, the spatiotemporal waveform became a solitary state, which was a periodic but distorted sine wave. In this case, the two-dimensional power spectrum showed a standard coherent mode and its high harmonics. When the magnetic field was over 0.03 T (electron/ion gyro radii are 0.14 mm/6.8 mm) and the argon pressure was under 3 mTorr, the spatiotemporal waveform became a turbulent regime. Especially when the magnetic field was around 0.09 T (electron/ion gyro radii are 46 μm/2.3 mm) and the argon pressure was under 2 mTorr, the fluctuation was strongly localized in the poloidal direction which means a streamer structure was appeared in the spatiotemporal waveform.

Figure 1(*a*) shows the spatiotemporal waveform of the ion saturation-current fluctuation at $r = 40$ mm in the laboratory frame with the axial magnetic field of 0.09 T and the argon pressure of 0.8 mTorr. The positive and negative poloidal direction correspond to the electron and ion diamagnetic drift directions, respectively. A clear bunching of waves in the poloidal direction is observed in the spatiotemporal waveform. While the dominant modes, which are the carriers of the streamer, have poloidal mode number $m = 2$–3 and frequency $f \sim 5$–7 kHz and propagate in the electron diamagnetic direction, the envelope structure of the bunching of waves has poloidal mode number $m = 1$ and frequency $f = 1.4$ kHz and propagates in the ion diamagnetic direction (at least in the laboratory frame). Figure 1(*b*) is the two-dimensional power spectrum $S(m, f)$ of the ion saturation-current fluctuation. The dominant modes in the electron diamagnetic direction are $(m, f) = (2, 6.8\,\text{kHz}), (3, 5.4\,\text{kHz}), (1, 3.4\,\text{kHz}), (4, 4.0\,\text{kHz}), (1, 8.2\,\text{kHz})$, and so on. From figure 1(*a*), it is clear that modes $(m, f) = (2, 6.8\,\text{kHz})$ and $(3, 5.4\,\text{kHz})$ are the fine structures in the spatiotemporal waveform and they are the carriers of the streamer structure. There also exists a large amplitude mode in the ion diamagnetic direction, $(m, f) = (1, -1.4\,\text{kHz})$. Its poloidal mode number and frequency agree with the poloidally localized envelope structure of the streamer, and it is called 'mediator' of the streamer formation. The coincidence of the properties of the mediator and envelope is explained by the nonlinear couplings between the mediator and carrier modes. The mediator nonlinearly couples with drift wave (quasi-)modes such as $(m, f) = (2, 6.8\,\text{kHz})$ and creates another quasi-modes such as $(m, f) = (3, 5.4\,\text{kHz})$. The two modes $(m, f) = (2, 6.8\,\text{kHz})$ and $(3, 5.4\,\text{kHz})$ make a beat wave, of which the poloidal mode number and frequency are the same as the mediator mode.

The bi-phase of the three modes derived by the bi-spectral analysis indicates the phase difference between the mediator mode and envelope structure. By recent studies, the two-dimensional cross-sectional phase structures of the mediator and envelope were analysed. While the envelope of the streamer had an elongated structure in the radial direction, the radial phase profile of the mediator had a jump at the middle of the plasma cross section. These features were quite equivalent with a pair of fast and slow modes predicted by a nonlinear Schrödinger equation based on the Hasegawa–Mima model [18]. The fast and slow modes correspond to the streamer structure and mediator, respectively. Such kind of a streamer structure, accompanied with a mediator, was also observed in a nonlinear simulation of drift waves in linear plasmas, using a three-field reduced fluid model [19].

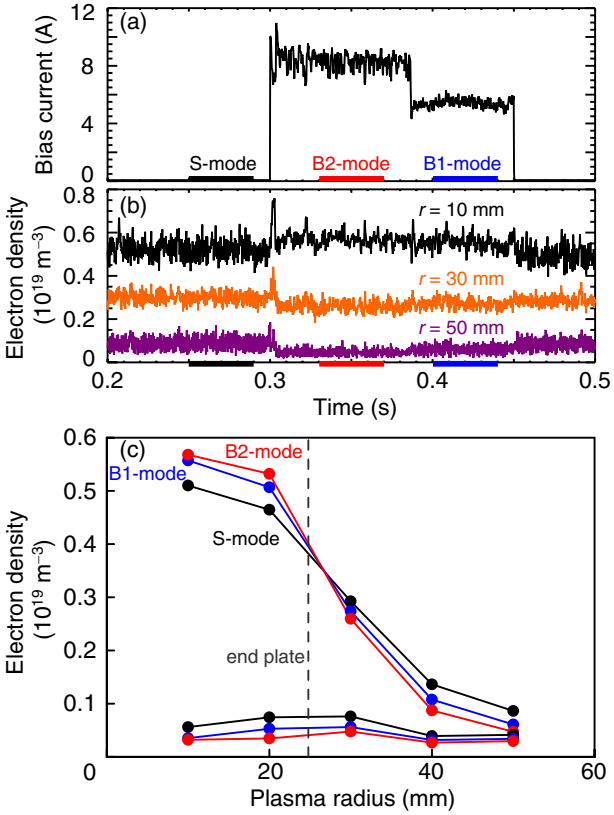

Figure 2. Time evolutions of (*a*) bias current and (*b*) electron density at $r = 10$, 30 and 50 mm when 50 V of bias voltage was applied. (*c*) Radial profiles of average electron density and absolute density fluctuation level in S-mode (black), B1-mode (blue) and B2-mode (red). Each time is indicated in (*a*) and (*b*) with lines.

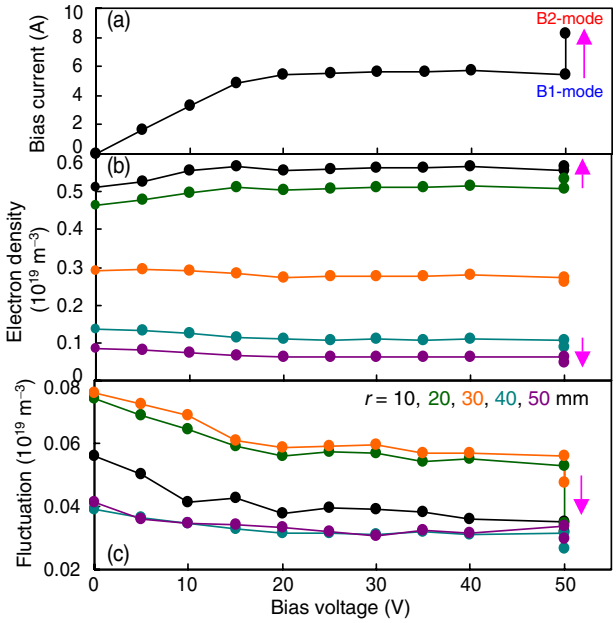

Figure 3. Bias voltage dependencies of (*a*) bias current, (*b*) average electron density and (*c*) absolute density fluctuation. (*b*) and (*c*) show data of five radial positions, $r = 10$, 20, 30, 40 and 50 mm.

3. End plate biasing

The meso-scale streamer structure is a radially elongated structure. Therefore, it is expected to enhance the radial transport which results in poor plasma confinement. The quantification of the effect on the plasma radial transport by streamers is now ongoing, however, in this paper the suppression study of the streamer is the main topic. The plasma source region has an inner diameter of 95 mm and the plasma diameter is around 100–120 mm. We located an end plate with a diameter of 50 mm, which was no larger than half of the plasma diameter, near the dead end of the PANTA vacuum vessel ($z = 3950$ mm). The positive biasing up to 50 V, which was the limit of the power supply capability for the current experimental facilities, was applied to the streamer (S)-mode (the same discharge condition as figure 1, i.e., magnetic field of 0.09 T and argon pressure of 0.8 mTorr) of the PANTA plasma. The aim of this experiment was to verify the suppression of the fluctuation level and destruction of the steamer structure by inducing a large radial electric field at around $r = 25$ mm. The end plate bias was applied from 0.30 to 0.45 s during each discharge (pulse length was 0.5 s). The bias current I_b (A) was monitored. The spatiotemporal waveform of the ion saturation-current at $r = 40$ mm and $z = 1885$ mm was measured with the 64-channel poloidal probe array. In addition, the electron density and floating potential profiles were measured with the five-channel radial probe array located at $r = 10$, 20, 30, 40 and 50 mm and $z = 1625$ mm, just in front of the 64-channel probe array.

Figures 2(*a*) and (*b*) are examples of the discharge with the biasing of 50 V, and they show the time evolutions of the bias current and electron density at $r = 10$, 30 and 50 mm. When the bias voltage was 50 V, the bias current took two values and jumped from one to the other several times during biasing. The lower value was 5.5 A, which we called the biased 1 (B1)-mode, and the higher value was 8.5 A, the biased 2 (B2)-mode. This phenomenon occurred almost every time when the bias voltage was 50 V and hardly occurred when that was under 40 V. For the discharge shown in figure 2, the plasma shifted to B2-mode immediately after applying the bias of 50 V at 0.3 s, transited to B1-mode at 0.39 s and remained in B1-mode until the biasing ended at 0.45 s. The state transition occurred only once with this discharge, however, usually the transition occurred several times within one discharge. Figure 2(*c*) shows the radial profiles of the average electron density and absolute density fluctuation in S-mode, B1-mode and B2-mode. From figures 2(*b*) and (*c*), it can be seen that the average electron density at $r = 10$ and 20 mm (inside the end plate region) increased in B1-mode and further increased in B2-mode, while that at $r = 30$ mm did not change significantly and those at $r = 40$ and 50 mm (outside the end plate region) decreased. The radial electron density profile became more peaked in B1-mode compared to the non-biased S-mode, and became rather more peaked profile in B2-mode. The absolute electron density fluctuation decreased during the biasing at all radii, meaning that the electron density fluctuation was suppressed and the suppression in B2-mode was stronger than that in B1-mode.

Figure 3 shows the biasing voltage dependencies of the bias current, average electron density and absolute electron density fluctuation. As shown in figure 3(*a*), the bias current linearly increased until the bias voltage V_b (V) reached 15 V

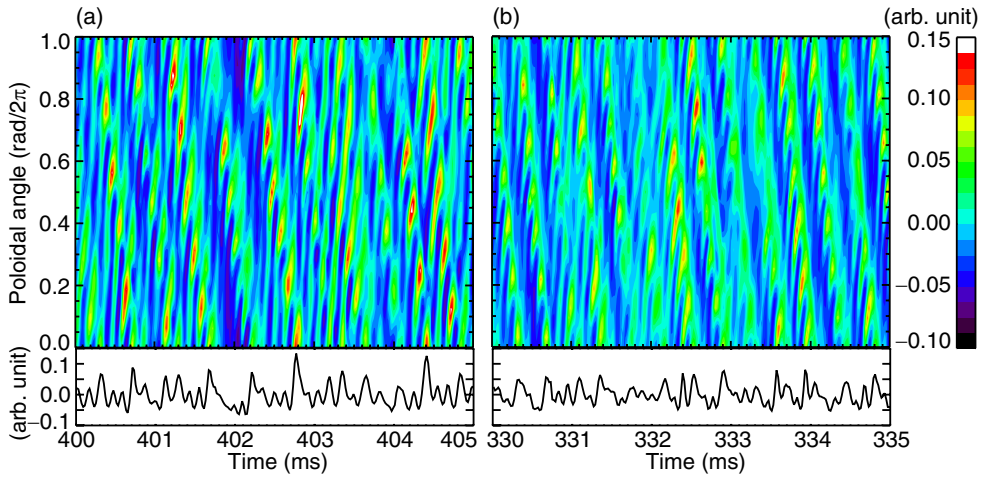

Figure 4. Spatiotemporal waveforms (with temporal waveforms at $\theta = 0$) of ion saturation-current fluctuation in (a) B1-mode and (b) B2-mode.

with the relation $I_b = V_b/3$. When the bias voltage exceeded 20 V, the bias current reached the electron saturation-current and was in the range of 5.5–6 A. However, when the bias voltage reached 50 V, it took two values, i.e., 5.5 A (B1-mode) and 8.5 A (B2-mode). Similarly to the bias current response, the average density and absolute density fluctuation stopped responding after the bias voltage exceeded 20 V but suddenly jumped when the state transited to B2-mode (see figures 3(b) and (c)). Without biasing, the absolute fluctuation levels were 6 m^{-3}, 7 m^{-3}, 8 m^{-3}, 4 m^{-3} and 4 $\times$ 10^{17} m^{-3} at $r = 10$ mm, 20 mm, 30 mm, 40 mm and 50 mm, respectively. The fluctuation level was suppressed linearly to the bias voltage until $V_b = 15$ V. The absolute fluctuation levels with $V_b = 20$ V were suppressed to ~70% at $r = 10$ mm and ~80% at the other radii. The suppression was almost constant from $V_b = 20$ V (B1-mode), but suddenly got strong to 60%, 50%, 60%, 70% and 70% at $r = 10$ mm, 20 mm, 30 mm, 40 mm and 50 mm, respectively, in B2-mode. These observations suggest that the fluctuation was suppressed during the biasing especially in the centre of the plasma (inside the end plate region). Although the reason of the transition between B1-mode and B2-mode is not understood yet, this interesting phenomenon leads to the future transition studies in linear plasmas.

Figure 4 shows the spatiotemporal waveform of the ion saturation-current fluctuation measured with the 64-channel poloidal probe array at $r = 50$ mm and $z = 1885$ mm. Compared to figure 1(a), the spatiotemporal waveform in B1-mode shows less features of the streamer structure; the poloidally localized structure is broken and the waveform is more periodic. In B2-mode, the poloidally localized structure disappeared and the waveform was almost in a periodic solitary state. Now we discuss about the deconstruction of the streamer structure. The streamer structure is radially elongated and has a strong radial connection. However, the radial electric field induced by the end plate biasing cut the radial connection and disturbed the construction of the streamer. To prove this hypothesis, the radial floating potential profile was measured with the five-channel radial probe array at $z = 1625$ mm. Not accurate but a rough tendency of the radial electric field can be derived just from the radial floating potential profile.

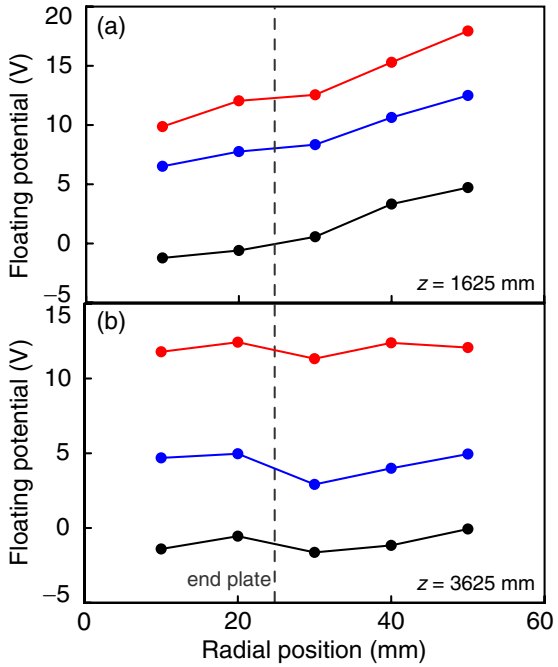

Figure 5. Radial floating potential profiles at axial positions of (a) 1625 mm and (b) 3625 mm for S-mode (black), B1-mode (blue) and B2-mode (red).

Figure 5(a) shows the radial floating potential profiles in S-mode, B1-mode and B2-mode. Just a shift of the floating potential during the biasing was observed. There is not much difference in the derivative of the floating potential profiles. It means that a strong radial electric field was not induced at $z = 1625$ mm during the biasing. Then, we focused to the change in the floating potential near the end plate. The five-channel radial probe array was moved near to the end plate. Figure 5(b) shows the radial floating potential profiles at $z = 3625$ mm in S-mode, B1-mode and B2-mode. This time, a strong radial electric field was induced at $z = 3625$ mm in B1-mode. Very rough radial electric field at $r = 25$ mm calculated from the derivative of the floating potential was -100 V m^{-1} in S-mode, increased the absolute value to -200 V m^{-1} in

B1-mode, but decreased to $-100\,\mathrm{V\,m^{-1}}$ in B2-mode. In this calculation, flat temperature profile was assumed. (Typical measured profiles are introduced in [15].) Temperature profile measurement during biasing is planned for more precise evaluation. The conclusion is that a strong radial electric field was induced by the end plate biasing near the end plate region. The strong plasma potential imposed to the plasma decayed towards the source region along the axial direction because of the resistivity of the plasma, so that the induced radial electric field was not observed other than the end plate region. However, the radial electric field at the end plate region deconstructed the streamer structure and since the axial correlation length of the plasma turbulence was very long (up to the device size) [4], the streamer structure was broken in all through the plasma. Thus, interaction between the streamer and radial electric field by external biasing was studied for the first time. But a question remains why the radial electric field in B2-mode decreased as low as the non-biased S-mode.

4. Summary

In summary, end plate biasing was applied to the streamer state in the PANTA linear plasma. Experimental results showed (i) new bifurcation phenomenon, (ii) profile steepening and fluctuation suppression during biasing and (iii) destruction of the streamer.

(i) New bifurcation phenomenon: The plasma response saturated when the bias voltage exceeded 20 V (the biased 1 (B1)-mode), however, when the bias voltage reached 50 V, the plasma entered to the biased 2 (B2)-mode and transited several times between B1-mode and B2-mode during the biasing. The radial electron density profile was steepened and the fluctuation was suppressed during B1-mode, and became much more peaked profile and the fluctuation was further suppressed when the plasma entered B2-mode.

(ii) Profile steepening and fluctuation suppression during biasing were observed. Compared to the non-biased state, the density profile became peaked in B1-mode and much peaked in B2-mode. The reduction rate of the density fluctuation was around 70–80% in B1-mode and 50–70% in B2-mode.

(iii) Destruction of the streamer: the poloidally localized structure was broken and became a solitary state during the biasing. The spatiotemporal waveform became almost periodic in B2-mode. The radial electric field induced near the end plate, which is possible to deconstruct the streamer structure, is changed. However, the radial electric field itself was not changed at the axial position far from the end plate because of the plasma resistivity. Since the axial correlation length was as long as the device length, the streamer structure was deconstructed all through the PANTA plasma.

Mechanisms of the electric field on the bifurcation and streamer destruction have not been clarified yet. Lower radial electric field in B2-mode than that in B1-mode is not solved. Further biasing experiments in PANTA would resolve these issues. Detailed turbulence study on a laboratory plasma is very beneficial to develop the turbulence control scenario in the toroidal plasmas.

Acknowledgments

This work was supported by Grants-in-Aid for Scientific Research of JSPS, Japan (21224014 and 25820434) and the collaboration programmes of NIFS (NIFS13KOCT001) and RIAM, Kyushu University.

References

[1] Fujisawa A. 2009 *Nucl. Fusion* **49** 013001
[2] Yamada T. *et al* 2008 *Nature Phys.* **4** 721
[3] Yamada T. *et al* 2010 *Phys. Rev. Lett.* **105** 225002
[4] Yamada T. *et al* 2008 *Plasma Fusion Res.* **3** 044
[5] Sasaki M. *et al* 2014 Dynamical response of turbulent structures in cylindrical magnetized plasmas *J. Phys. Soc. Japan* at press
[6] Taylor R.J. *et al* 1989 *Phys. Rev. Lett.* **63** 2365
[7] Weynants R.R. *et al* 1992 *Nucl. Fusion* **32** 837
[8] Inagaki S. 1997 *Japan. J. Appl. Phys.* **36** 3697
[9] Kitajima S. 2011 *Nucl. Fusion* **51** 083029
[10] Komori A., Watanabe K. and Kawai Y. 1988 *Phys. Fluids* **31** 210
[11] Schröder C. *et al* 2001 *Phys. Rev. Lett.* **86** 5711
[12] Shinohara S. and Matsuyama S. 2002 *Phys. Plasmas* **9** 4540
[13] Carter T.A. and Maggs J.E. 2009 *Phys. Plasmas* **16** 012304
[14] Moon C., Kaneko T. and Hatakeyama R. 2013 *Phys. Rev. Lett.* **111** 115001
[15] Oldenbürger S. *et al* 2012 *Plasma Phys. Control. Fusion* **54** 055002
[16] Oldenbürger S. *et al* 2012 *Plasma Phys. Control. Fusion* **7** 2401146
[17] Yamada T. *et al* 2007 *Rev. Sci. Instrum.* **78** 123501
[18] Nozaki K., Taniuti T. and Watanabe K. 1979 *J. Phys. Soc. Japan* **46** 991
[19] Kasuya N., Yagi M., Itoh K. and Itoh S.-I. 2008 *Phys. Plasmas* **15** 052302